

VLBI OBSERVATIONS OF THE NEARBY TYPE IIB SUPERNOVA 2011dh

M. F. BIETENHOLZ^{1,2}, A. BRUNTHALER^{3,4}, A. M. SODERBERG⁵, M. KRAUSS⁴, B. ZAUDERER⁵, N. BARTEL², L. CHOMIUK^{4,5,6},
AND M. P. RUPEN⁴

Accepted to the Astrophysical Journal

ABSTRACT

We report on phase-referenced VLBI radio observations of the Type Iib supernova 2011dh, at times $t = 83$ days and 179 days after the explosion and at frequencies, respectively, of 22.2 and 8.4 GHz. We detected SN 2011dh at both epochs. At the first epoch only an upper limit on SN 2011dh's angular size was obtained, but at the second epoch, we determine the angular radius SN 2011dh's radio emission to be 0.25 ± 0.08 mas by fitting a spherical shell model directly to the visibility measurements. At a distance of 8.4 Mpc this angular radius corresponds to a time-averaged (since $t = 0$) expansion velocity of the forward shock of 21000 ± 7000 km s⁻¹. Our measured values of the radius of the emission region are in excellent agreement with those derived from fitting synchrotron self-absorbed models to the radio spectral energy distribution, providing strong confirmation for the latter method of estimating the radius. We find that SN 2011dh's radius evolves in a power-law fashion, with $R \propto t^{0.92 \pm 0.10}$.

Subject headings: supernovae: individual (SN2011dh) — radio continuum: general

1. INTRODUCTION

Supernova SN 2011dh was discovered on 2011 May 31 by the amateur astronomer Amádée Riou in the nearby galaxy M51 (Griga et al. 2011), which is at a distance of 8.4 ± 0.6 Mpc (Feldmeier et al. 1997; Vinkó et al. 2012). The supernova was soon confirmed using pre- and post-discovery imaging (Griga et al. 2011). In particular the optical transient was also detected by the Palomar Transient Factory (Law et al. 2009) shortly after the initial discovery. The explosion date is tightly constrained to be between 2011 May 31.275 and 31.893 UT (Arcavi et al. 2011). We will adopt the (rounded) midpoint of this interval of $t_0 = \text{May } 31.6$ UT. The supernova was coincident with the eastern spiral arm of M51, and had an estimated apparent magnitude of ~ 14 mag (unfiltered) implying an absolute magnitude of roughly ~ -16 mag. We note that M51 is also host to an earlier supernova, SN 1994I, which however was of Type Ib/c.

Initially, SN 2011dh was spectroscopically classified as Type IIP (Silverman et al. 2011), but further spectroscopy, which showed helium absorption features, caused a re-classification as a Type Iib (Arcavi et al. 2011; Marion et al. 2011). A maximum expansion velocity of ~ 17000 km s⁻¹ was estimated from the blue edge of the H α line (Silverman et al. 2011; Arcavi et al. 2011).

Radio emission was detected on June 4, only a few days after the explosion, at centimeter wavelengths (Horesh et al. 2011a) with the National Radio Astron-

omy Observatory⁷ (NRAO) Expanded Very Large Array (EVLA; Perley et al. 2011), at millimeter wavelengths (Horesh et al. 2011b) using the Combined Array for Research in Millimeter-wave Astronomy (CARMA), and at sub-mm wavelengths (Soderberg et al. 2011) using the Submillimeter Array (SMA). The initial radio and mm-band observations were presented in Soderberg et al. (2011). Further radio flux-density measurements as well as modeling of the light curve are presented in a companion paper to the present one, Krauss et al. (2012).

Although a yellow supergiant star was identified on pre-explosion *Hubble Space Telescope* (*HST*) images as a possible progenitor (Van Dyk et al. 2011; Maund et al. 2011), subsequent work by Arcavi et al. (2011) suggested a smaller progenitor. Soderberg et al. (2011) examined the early data at radio through X-ray wavelengths and concluded that these also suggest a small progenitor star with a stellar radius of $\sim 10^{11}$ cm and were not consistent with a radius of order 10^{13} cm as would be expected for a yellow supergiant. The yellow supergiant identified in the *HST* images would then have to be either a binary companion of, or possibly a chance superposition with, the true progenitor star.

Chevalier & Soderberg (2010) proposed that Type Iib supernovae (SNe Iib) are divided into two distinct subclasses. The first, SN cIib, have compact progenitors, with stellar radii $\sim 10^{11}$ cm, (e.g., SN 2001ig, Ryder et al. 2004; SN 2003bg, Soderberg et al. 2006; and SN 2008ax, Roming et al. 2009). They are characterized by high shock velocities of $\sim 0.1 c$, and radio light curves which show deviations from a power-law decay at late times. The second, SN eIib, (e.g., SN 1993J, Bartel et al. 2002; SN 2001gd Pérez-Torres et al. 2005) have extended progenitors, with stellar radii $\sim 10^{13}$ cm, and are characterized by somewhat slower shock velocities and smooth radio light curves.

The size and expansion velocity of the shockfront is a

¹ Hartebeesthoek Radio Observatory, PO Box 443, Krugersdorp, 1740, South Africa

² Department of Physics and Astronomy, York University, Toronto, M3J 1P3, Ontario, Canada

³ Max-Planck-Institut für Radioastronomie, Auf dem Hügel 69, 53121 Bonn, Germany

⁴ National Radio Astronomy Observatory, Socorro, NM 87801, USA

⁵ Harvard-Smithsonian Center for Astrophysics, 60 Garden Street, Cambridge, MA 02138, USA

⁶ Jansky Fellow of the National Radio Astronomy Observatory

⁷ The National Radio Astronomy Observatory is a facility of the National Science Foundation operated under cooperative agreement by Associated Universities, Inc.

basic characteristic distinguishing different supernovae, and it is therefore important to determine it observationally as directly as possible. In particular, to determine whether SN 2011dh conforms to the characteristics of Chevalier & Soderberg’s proposed Type SN cIIb class requires measuring the expansion velocity of the shock front. Very long-baseline-interferometry (VLBI) observations are the most direct way of making this measurement (see e.g., Bietenholz et al. 2010; Brunthaler et al. 2010; Bietenholz 2008). Unlike the optical emission, which mostly originates in the denser and more slowly moving inner ejecta, the radio emission generally traces the fastest ejecta. The radio emission is thought to originate in the region between the forward and reverse shocks. In the particularly well-studied case of SN 1993J, Bartel et al. (2007) show that there is a close relationship between the outer boundary of the radio emission and the location of the forward shock.

However, even with the high resolution afforded by VLBI, it is generally difficult to measure the radius of the radio-emitting region, and thus of the forward shock, especially early on in the evolution of a supernova when its size is still small. Chevalier (1998; see also Chevalier & Fransson 2006) has shown that, for a supernova spectrum dominated by synchrotron self-absorption (SSA), the radius of the emitting region, R , (assumed spherical), as well as the magnetic field can be determined from two observable quantities: the frequency and spectral luminosity of the peak in the radio spectral energy distribution (SED). The observables require only measurements of the total flux density at different frequencies, and thus are not dependent on spatially resolving the supernova. In the case that significant free-free absorption is present in addition to SSA, a lower limit on the shockfront radius is obtained.

This calculation of the radius is fairly robust. However, in addition to the mentioned observables and the distance, D , which is usually fairly well constrained, the calculation does also rely on assumed values for two poorly known parameters. The first of these, f , is the filling factor of the radio emission, while the second⁸, ψ , is the ratio of relativistic electron energy density to magnetic energy density in the post-shock region.

In the case of SN 2011dh, Soderberg et al. (2011) showed that the cm and mm-wave radio flux densities are consistent with a synchrotron self-absorbed spectrum at $t \simeq 5$ and 17 days, and determined that $R \simeq 3.7 \times 10^{15}$ cm at the latter epoch. In our companion paper, Krauss et al. (2012) continue this work through to $t = 92$ days, and present detailed EVLA monitoring of the multi-frequency radio light curves, as well as modeling the light curves to show that the evolution of R , as calculated from the radio SED, is consistent with a power-law evolution with $R \propto t^{0.9}$.

We report in this paper on VLBI observations of SN 2011dh obtained at $t = 83$ and 179 days after the explosion, which have allowed us to directly measure (or at least constrain) the angular size of SN 2011dh at those epochs. Early results from the first set of observations have already been reported in Bietenholz et al. (2011b).

⁸ Note that Krauss et al. (2012), Soderberg et al. (2011) and Chevalier (1998) use the symbol α for this parameter, which symbol we use here to denote the radio spectral index.

2. RADIO LIGHT CURVES

To set the context for, and aid in the interpretation of, the VLBI results, we present in Figure 1 the radio light curves of SN 2011dh at 22.2 and 8.4 GHz, the two frequencies at which we carried out the VLBI observations. The flux density values at 22.2 GHz were logarithmically interpolated in frequency between 20.5 and 25.0 GHz from those presented in Krauss et al. (2012), with the exception of the last one at $t = 183$ days. For that last one, we obtained additional EVLA observations on 2011 November 30 at 20.5 and 25 GHz. The data reduction procedure was as described in Krauss et al. (2012). We obtained flux densities of $722 \pm 72 \mu\text{Jy}$ at 20.5 GHz and $551 \pm 55 \mu\text{Jy}$ at 25 GHz, with the uncertainties being intended as standard errors and dominated by an estimated 10% systematic contribution. The value for the flux density at the time of the 22.2-GHz VLBI observations at $t = 92$ days was then interpolated logarithmically first in frequency and then in time between the adjacent values.

The 8.4-GHz measurements were also taken from Krauss et al. (2012). Near the time of the second VLBI observations, the VLA was in the compact D array configuration, with resolution insufficient to overcome confusion at 8.4 GHz, so a direct measurement could not be obtained. We therefore estimated the 8.4-GHz flux density by first interpolating the 22.2-GHz values logarithmically in time to $t = 179$ days, and then extrapolating to 8.4 GHz by assuming the same radio spectral index of $\alpha = -1$ (where $S_\nu \propto \nu^\alpha$) as was found appropriate for the optically thin part of the spectrum through to $t = 92$ days (Krauss et al. 2012). Although the optically-thin spectral index has been seen to vary with time in some supernovae (e.g., Bartel et al. 2002; Bartel & Bietenholz 2008), large variations are not expected, so there is no reason to think the model of Krauss et al. (2012) can not be extrapolated to $t = 179$ days, so our estimate of the 8.4-GHz flux density at that time is of sufficient accuracy for comparing to the flux density recovered from the VLBI observations.

3. VLBI OBSERVATIONS

Our two sessions of VLBI imaging observations of SN 2011dh were carried out using the high-sensitivity array, which consisted of the NRAO Very Long Baseline Array (VLBA; 10×25 -m diameter, distributed across the United States), the NRAO Robert C. Byrd (~ 105 m diameter) telescope and the Effelsberg (100 m diameter) telescope. Both sessions were 13 hr in length, with the first using an observing frequency of 22.2 GHz on 2011 August 21 UTC, and the second using an observing frequency of 8.4 GHz on 2011 November 26 UTC. The age of the supernova was 83 and 179 days, respectively, at the midpoints of our two sessions.

In each set of observations, we included several “geodetic blocks,” where we observed 12–15 bright sources from the International Celestial Reference Frame (ICRF) list of sources (Fey et al. 2009) over a period of ~ 45 minutes to measure the tropospheric zenith delay and clock offsets at each antenna (see Brunthaler et al. 2005; Reid & Brunthaler 2004). In these geodetic blocks we recorded 8 intermediate frequencies (IFs) with frequency centers spread over a ~ 400 MHz range, with each IF

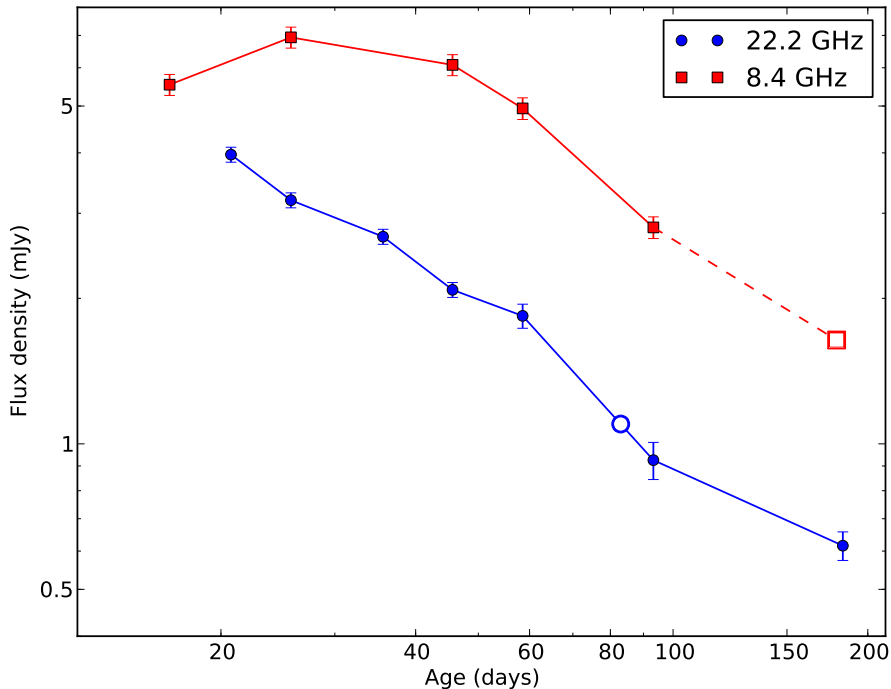


Figure 1. Radio light curves of SN 2011dh at 22.2 and 8.4 GHz, as obtained from EVLA observations. Flux density measurements are shown by solid circles and squares. See text for details of how the flux density values were obtained. With the exception of the one at age = 183 days, they were taken or interpolated from Krauss et al. (2012). The open square represents the interpolated value at our first VLBI observing date and frequency (22.2 GHz at age = 83 days) while the open circle and dashed line show the extrapolation to our second VLBI session (8.4 GHz at age = 179 days). The age of the supernova is calculated from the explosion date of 2011 May 31.6 UT.

covering a bandwidth of 8 MHz.

For the observations of SN 2011dh we recorded a contiguous bandwidth of 64 MHz in each of the two senses of circular polarization with two-bit sampling⁹, for a total bit rate of 512 Mbit s⁻¹. We used J1332+4722 (ICRF J133245.2+472222), 0^o5 away from SN 2011dh, as a primary phase calibrator. This source is an ICRF source (Fey et al. 2009) with a position known to $\sim 70 \mu\text{as}$. Any positions in this paper are calculated by taking the position of J1332+4722 to be RA = 13^h 32^m 45^s.24642, decl. = 47^o 22' 22".6670 for J1332+4722. For the first session, at 22 GHz, we used a cycle time of ~ 110 s, with ~ 60 s duration on SN 2011dh and ~ 50 s on J1332+4722, while for the second session at 8.4 GHz, we used a somewhat longer cycle time of ~ 170 s, with ~ 120 s spent on SN 2011dh.

We considered as a possible phase-reference source the weak nuclear radio source of M51 (Maddox et al. 2007), which is only $\sim 3'$ from SN 2011dh. This nuclear source, however, has a low 5-GHz peak brightness of < 1 mJy, as well as having a steep spectral index, and is therefore too weak to use for phase referencing at our observing frequencies of 8.4 and 22.2 GHz.

During each of the observing runs, we also spent three ~ 20 -m periods observing an astrometric “check” source,

⁹ We note that parallel recordings were made using the higher bandwidth of 256 MHz per polarization, corresponding to a bit rate of 2 Gbit s⁻¹, with the experimental new Mark 5C recording units. Various technical difficulties with these recordings, however, rendered the correlated data unreliable, and we base the results in this paper only on the data recorded at 512 Mbit s⁻¹ using the well-tried Mark 5B recording systems.

the quasar JVAS J1324+4743, which was about 1^o5 away from our primary phase-reference source J1332+4722. The purpose of the observations of J1324+4743 was to check the quality of the phase-referencing and also to provide a second astrometric reference source. This check source was observed using a similar phase-referencing pattern as we used for SN 2011dh.

The VLBI data were correlated with the DiFX correlator (Deller et al. 2011), and the analysis carried out with NRAO’s Astronomical Image Processing System (AIPS) and ParselToungue (Kettenis et al. 2006). We calibrated both sets of observations using standard procedures, making a correction for the dispersive ionospheric delay using the AIPS task TECOR, and solving for the zenith tropospheric delay on the basis of our geodetic-block observations. We discarded any SN 2011dh visibility data obtained when either of two the antennas involved was observing at elevations below 10^o.

The initial flux density calibration was done through measurements of the system temperature at each telescope, and then improved through self-calibration of the primary reference source J1332+4722. This source is slightly resolved, as can be seen on the images in the VLBA calibrator list data-base¹⁰, where a weak extension or second component is visible ~ 2 mas to the west-southwest of the peak. We see a similar structure in the images made from our data at both 22 and 8.4 GHz. Our final amplitude and phase calibration at both frequencies was derived using a CLEAN model of this source,

¹⁰ <http://www.vlba.nrao.edu/astro/calib>

with the peak-brightness point in the image being placed at the nominal coordinates given above¹¹. Finally this calibration was interpolated to the intervening scans of SN 2011dh.

4. RESULTS

4.1. Results from the 2011 August 24 Observations at 22 GHz

Unfortunately, the weather was generally poor for our first set of observations, at 22 GHz, resulting in higher than usual noise levels: the rms background brightness in a naturally-weighted image was $92 \mu\text{Jy beam}^{-1}$. Nonetheless SN 2011dh was clearly detected, with a peak brightness of $630 \mu\text{Jy beam}^{-1}$, which was 6.8 times the rms background. As mentioned above, early results from this epoch were reported in Bietenholz et al. (2011b).

For marginally resolved sources, such as SN 2011dh, the best values for the source size and VLBI flux density come from fitting models directly to the visibility data, rather than from imaging. We chose as a model the projection of an optically-thin spherical shell of uniform volume emissivity, with an outer radius of $1.25\times$ the inner radius¹². Such a model has been found to be appropriate for other radio supernovae (see e.g., Bietenholz et al. 2003; Bartel & Bietenholz 2008). The Fourier transform of this shell model is then fitted to the visibility measurements by least squares. For a partially resolved source such as SN 2011dh, the exact model geometry is not critical, and our shell model will give a reasonable estimate of the size of any circularly symmetric source, with a scaling factor of order unity dependent on the exact morphology (see discussion in Bartel et al. 2002).

For the observations of SN 2011dh at $t = 83$ days, our best-fit spherical shell model had a total flux density of $650 \pm 140 \mu\text{Jy}$ (statistical and systematic uncertainty combined). We note that the total flux density as interpolated from the VLA measurements was $1100 \mu\text{Jy}$ (see Section 2 and Figure 1), with an estimated uncertainty of 10%, and is therefore higher than that recovered from the VLBI observations by a combined 2.5σ . This discrepancy suggests that there is likely some loss of phase-coherence in the VLBI observations, which is not unexpected given the relatively poor weather.

We obtained a value of $0.11_{+0.09}^{-0.11}$ mas for the outer angular radius of SN 2011dh at this epoch, where the listed uncertainty is intended as a standard error, and consists of both the statistical and systematic components added in quadrature. We estimated the systematic component as follows: the largest systematic error most likely arises from the uncertainty in the antenna amplitude gains, which are only imprecisely known but are correlated with the fitted source size for marginally resolved sources, as well as from the likely coherence losses

¹¹ The deviation of the source geometry of J1332+4722 from a point source is small enough so that the effect of using a point model in the solutions for delay and delay rate made using FRING solutions is negligible.

¹² Our results do not depend significantly on the assumed ratio between inner and outer radii, as the effect of reasonable variations in this ratio is considerably less than our stated uncertainties. For a discussion of uncertainties on the shell-size obtained through u - v plane model-fitting compared with those obtained in the image plane for the case of SN 1993J, showing that superior results are obtained using the former, see Bietenholz et al. (2011a).

mentioned above. Although the effect of the latter is difficult to estimate reliably, the first order effect would be a reduction in the visibility amplitude. We accordingly estimated the effects of both amplitude-gain errors and coherence loss from a small Monte-Carlo simulation where we randomly varied the amplitude gains of the individual telescopes by 20% rms, to arrive at the uncertainty in the angular radius listed above. The supernova is therefore not significantly resolved at this epoch, and the 3σ upper limit on the outer radius was 0.38 mas.

We also take the fitted center position of the model as our best estimate of the center-position of SN 2011dh. For this epoch, this position was RA = $13^{\text{h}} 30^{\text{m}} 5^{\text{s}}.105548$ and decl. = $47^{\circ} 10' 10''.92273$. The statistical uncertainty on this position is $\sim 50 \mu\text{as}$, however, a realistic position uncertainty will have substantial contributions from unmodeled effects of the troposphere, ionosphere, station position errors, and possible evolution of the reference sources. We estimate the total uncertainty in the position relative to that of J1332+4722 to be $\sim 70 \mu\text{as}$. Our measured position therefore agrees to within less than the combined uncertainties with that measured by Martí-Vidal et al. (2011) at $t = 14$ days.

4.2. Results from the 2011 November 26 Observations at 8.4 GHz

In the second set of VLBI observations at 8.4 GHz, SN 2011dh was detected with good signal-to-noise ratio. We show the VLBI image of SN 2011dh in Figure 2. The fitted FWHM size of the CLEAN beam was 0.72×0.51 mas at p.a. -30° . For presentation we slightly super-resolved the image by restoring with a round clean beam of FWHM 0.51 mas. We emphasize that our measurement of the angular size of SN 2011dh, as presented below, is entirely independent of this super-resolution. The peak brightness in this image was $1160 \mu\text{Jy beam}^{-1}$, while the rms background brightness was $22 \mu\text{Jy beam}^{-1}$.

Since SN 2011dh is only partly resolved, we again turn to fitting models directly to the visibility measurements in order to accurately measure the size of the source. Due to the good signal-to-noise ratio obtained at this epoch, the source size could be fairly accurately constrained by this method. In the model-fitting, we used the square-root of the uncertainties of the visibility measurements, which procedure, though statistically less efficient, increases the robustness of results in the likely case that the errors in the visibility measurements are not purely statistical. We again used a spherical shell model with an outer radius 1.25 times the inner radius.

From the model-fitting, we obtained a total flux density of $1540 \pm 190 \mu\text{Jy}$ (an almost identical value was obtained from imaging). This value is only 7% below that of 1.64 mJy extrapolated for this epoch and frequency from the EVLA measurements (see Section 2 and Figure 1), although we note that the extrapolation EVLA value is somewhat uncertain in that it depends on the errors in the individual flux density measurements as well as the assumption that the radio spectral index does not vary in time. We find therefore that the flux density recovered from the VLBI measurements is in reasonable agreement with that extrapolated from the EVLA measurements, and that there is no reason to suspect significant correlation losses.

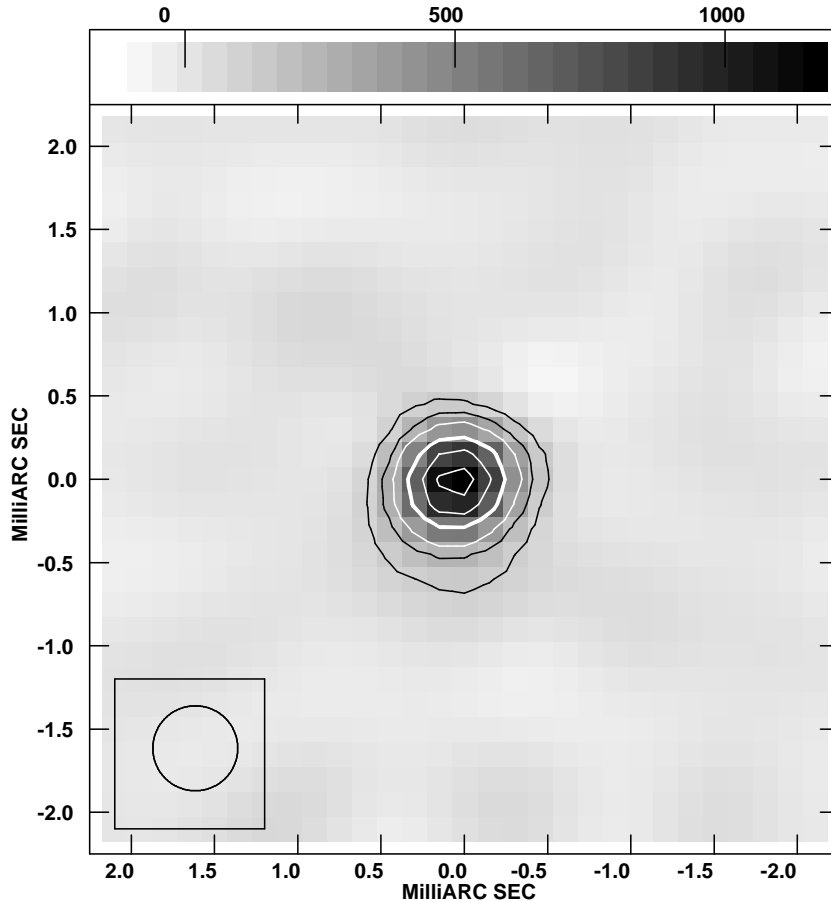


Figure 2. The CLEAN image of SN 2011dh made from VLBI observations at 8.4 GHz on 2011 November 26 UTC. To obtain more robust imaging, we started with the square root of the visibility weights and then used uniform weighting. The fitted CLEAN beam FWHM was 0.72×0.51 mas at p.a. -30° , and we super-resolved slightly by using a round CLEAN beam with FWHM of 0.51 mas, indicated at lower left. The contours are drawn at 10, 20, 30, 50, 70 and 90% of the peak brightness, with the 50% contour being emphasized. The peak brightness was $1160 \mu\text{Jy beam}^{-1}$, and the background rms brightness was $22 \mu\text{Jy beam}^{-1}$. The greyscale is labeled in $\mu\text{Jy beam}^{-1}$. North is up and east is to the left, and the coordinate origin is at the fitted center position of SN 2011dh, which was at RA $13^{\text{h}} 30^{\text{m}} 05^{\text{s}}.105548$, decl. $47^\circ 10' 10''.92273$.

We again also obtained a center position of SN 2011dh from this fit, which was consistent within the uncertainties with that obtained for our first epoch as well as with the position obtained at $t = 14$ days by Martí-Vidal et al. (2011). The formal difference in position over the 165-day interval between the Martí-Vidal et al. observation and the present one was $110 \pm 125 \mu\text{as}$.

Finally, we obtained an outer radius for SN 2011dh of 0.25 ± 0.08 mas, with the uncertainties again including both statistical and systematic contributions and derived as in the previous section. At a distance of 8.4 Mpc, this angular radius corresponds to an average expansion velocity since the explosion of $21000 \pm 7000 \text{ km s}^{-1}$.

To determine the quality of the phase referencing, upon which the above determinations of the position and angular radius depend, we examined the observations of our check source, J1324+4743. From the strictly phase-referenced data for the check source we found a total flux density of 101 mJy, while for the phase self-calibrated data we found a 36% higher value of 137 mJy. We fitted an elliptical Gaussian model, appropriate for a marginally resolved QSO, directly to the visibilities in a similar fashion as the shell model was fit to the SN 2011dh data. When fitting the strictly phase-

referenced data, we found that the fitted FWHM major axis was 25% larger than when we fit to the phase self-calibrated data. This implies that, at least in the case of our check source J1324+4743, the coherence losses due to phase-referencing can result in an error of 25% on the source size. We note however, that J1324+4743 was almost three times farther from the phase-reference source (J1332+4722) than was SN 2011dh. Furthermore, the u - v coverage for J1324+4743 was much poorer since we only observed it for three brief periods. We expect therefore that the additional errors in the size of SN 2011dh due to coherence loss are considerably smaller than 25%, and thus considerably smaller than the uncertainties from other causes discussed above. We do not, therefore, find any reason to suspect that coherence losses due to poor phase-referencing would substantially increase the uncertainty we give above for the angular size of SN 2011dh.

5. DISCUSSION

We obtained VLBI observations of the nearby Type IIb supernova 2011dh, with the primary goal of obtaining a direct observational constraint on the expansion speed by measuring the angular size of SN 2011dh. VLBI observations are crucial, as they are the only means to directly

measure the size, expansion speed and perhaps the geometry of the radio emission region. We obtained an upper limit on the radius of SN 2011dh at $t = 83$ days and a measurement of the radius at $t = 179$ days. We plot these two values as a function of time in Figure 3 (red squares).

As mentioned in the introduction, the radius of a supernova can also be calculated from broadband, but not spatially-resolved, observations of the radio SED (spectral energy distribution), under the assumption of a spectrum dominated by SSA (synchrotron self-absorption). In our companion paper Krauss et al. (2012; see also Soderberg et al. 2011) we used such observations of the SED to calculate the shockfront radius for SN 2011dh through to $t = 92$. In particular, the radius is calculated following Chevalier & Fransson (2006; see also Chevalier 1998):

$$R = 4.0 \times 10^{14} \psi^{-1/19} \left(\frac{f}{0.5}\right)^{-1/19} \left(\frac{S_{\nu_{\text{op}}}}{\text{mJy}}\right)^{9/19} \times \left(\frac{D}{\text{Mpc}}\right)^{18/19} \left(\frac{\nu_{\text{op}}}{5 \text{ GHz}}\right)^{-1} \text{ cm}, \quad (1)$$

where $S_{\nu_{\text{op}}}$ is the observed flux density at the peak of the synchrotron spectrum, which occurs at frequency ν_{op} , D is the distance, and f and ψ are, as mentioned above, the filling factor and the ratio of the energy density in relativistic particles to that of the magnetic field, respectively.

For f we have some observational constraints at least in the well-studied case of another SN IIB, SN 1993J, where the well-resolved VLBI images suggest a very spherical shell structure with a shell thickness of 20% to 33% of the outer radius (e.g., Bartel et al. 2002; Bietenholz et al. 2011a; Martí-Vidal et al. 2010). Such a geometry would have a gross value of f in the range of 49% to 70%, although it is possible that small scale clumpiness within this overall geometry could reduce f below those values. For ψ , the commonly used value is $\psi = 1$, corresponding to equipartition. Here, and in our companion paper (Krauss et al. 2012) we therefore take $f = 0.5$ and $\psi = 1$.

The radius of SN 2011dh's forward shock was calculated from the SED as obtained from EVLA and SMA observations using this method at various times between $t = 4$ and 92 days by Soderberg et al. (2011) and Krauss et al. (2012). We plot these values also in Figure 3 (green circles).

Assuming that the supernova ejecta and circumstellar material have power-law density profiles, then evolution of the forward shock radius with time follows a power-law form and can be expressed simply as $R \propto t^m$, where m is known as the deceleration parameter. If the circumstellar density is, as expected for a stellar wind, $\propto R^{-2}$, and the outer portions of the ejecta are also characterized by a power-law density distribution with index n , then it can be shown that $m = (n - 3)/(n - 2)$ (Chevalier 1982). Indeed, we found in Krauss et al. (2012), that at least up to $t = 92$ days the evolution of SN 2011dh's radius was consistent with $m = 0.9$, implying that $n \simeq 12$.

In order to determine m from our various measurements of SN 2011dh's radius, we performed a weighted least-squares fit to the complete set of values for R , in-

cluding both those determined from our VLBI measurements and those from fitting the SED. The fitted line is also plotted in Figure 3 (in blue). As can be seen in Figure 3, the expansion of SN 2011dh is in fact well described by a power-law. The fit gives $m = 0.92 \pm 0.03$ and a radius at $t = 30$ days of $(5.85 \pm 0.13) \times 10^{15}$ cm, where the uncertainties are statistical ones derived from the scatter of the fit.

In addition to the power-law nature of the expansion, it can be seen from Figure 3 that there is excellent agreement between the radii measured with VLBI with those calculated from the radio SED under the assumption of SSA. This agreement provides strong validation for the latter method of calculating the shockfront radius. Indeed, SN 2011dh represents so far the best example for directly comparing the radii of the shock wave determined in these two different fashions.

The radii derived from fits to the SED are uncertain due to a number of systematic factors. Firstly, they are calculated from the fitting of a model SSA spectrum to the observed flux density values. In the case of SN 2011dh, although the SSA model is an excellent fit over a wide spectral range, the fit is not exact (see e.g., Krauss et al. 2012), resulting in estimated systematic uncertainties of 15% and 5%, respectively, on the values of ν_{op} and $S_{\nu_{\text{op}}}$, which result in a $\sim 15\%$ systematic uncertainty on the calculated radius. In Figure 3, the plotted error bars, intended as standard errors, include this systematic component on the values of R calculated from the SED. We performed a Monte-Carlo simulation where we varied all the radius measurements according to their standard errors, and found an rms scatter of the derived values of m of 0.10. It can be seen, however, that any such systematic errors do not seem time-dependent, in other words likely have only a small effect on the derived value of m . We therefore conservatively estimate the systematic 1σ uncertainty on our fitted value of m at 0.10.

The radii calculated from the SED also depend, as noted above, on the poorly known parameter ψ , for which we took the equipartition value of unity. Soderberg et al. (2011), however, found that for SN 2011dh the X-ray measurements, in conjunction with those in the radio, suggested deviations from equipartition, with $\psi \sim 30$. Can we constrain ψ by comparing the values of the R as calculated from the SED with those from VLBI which are independent of ψ ?

As can be seen from Equation 1 above, the former values of R in fact depend only weakly on ψ . In particular, the change of ψ from our assumed value of unity to $\psi = 30$, as suggested by Soderberg et al. (2011), would decrease the calculated values of R by 16%, producing only a small change in Figure 3. Using such slightly lower values of the R determined from the SED (but with the original values of R from VLBI) does not change the fitted value of m by more than the statistical uncertainty, and results in a slightly, but not significantly, poorer fit of the power-law expansion. We therefore conclude that the measurements are not yet of sufficient accuracy to usefully constrain ψ .

As we have shown, the deceleration parameter, m , for SN 2011dh seems robustly determined at $m \simeq 0.9$, which implies only slightly decelerated expansion, and consequently a relatively steep radial density profile in the

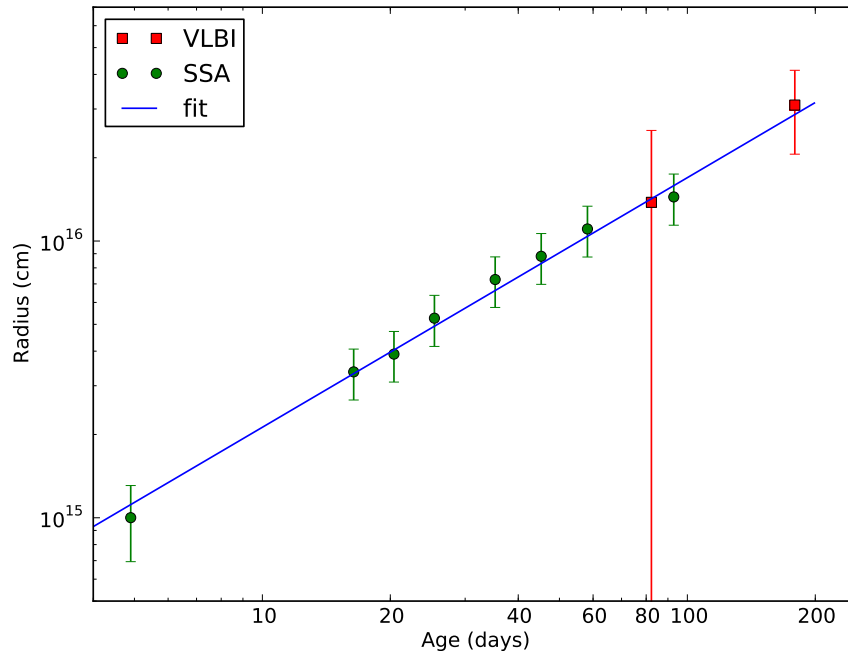


Figure 3. The shock front radii of SN 2011dh as estimated by two independent methods. In red, we plot the values derived from fitting spherical shell models to the VLBI visibility-data from this paper. The plotted 1σ error bars include statistical and systematic contributions (see text Section 3 for details). In green, we plot the values calculated from the radio spectral energy distribution under the assumption that it is dominated by SSA (synchrotron self-absorption), with the radius values taken from Soderberg et al. (2011) and Krauss et al. (2012), again with uncertainties including statistical and systematic components. The blue line represents our power-law fit to all the values, with $R = 5.85 \times 10^{15} (t/30 \text{ days})^{0.92} \text{ cm}$ (see text).

outer ejecta, with power-law index $n \simeq 12$. We note that Chevalier (1982) found that for self-similar models with $m = 0.9$ and $n = 12$ the ratio of outer shock to inner shock radii was 1.24, almost identical to our adopted value of 1.25.

The deceleration of SN 2011dh may show a pattern similar to that seen for SN 1993J, where $m \simeq 0.9$ was found for approximately the first year (Bartel et al. 2002; Martí-Vidal et al. 2010), albeit with somewhat smaller velocities than SN 2011dh. We note that the expansion velocities SN 2011dh’s shock front, as determined from the radio emission, are approximately twice as large as the highest velocity of $\sim 17000 \text{ km s}^{-1}$ observed in the optical spectrum (from the blue edge of the $H\alpha$ emission line; Silverman et al. 2011; Arcavi et al. 2011). This is not unexpected as the high-velocity shocked H is likely to be non-radiative (Chevalier & Soderberg 2010), and the ejecta should be characterized by a steep density profile (Berger et al. 2002; Chevalier & Fransson 2006).

Our observations also constrain the proper motion of the geometrical center of SN 2011dh: between the EVN observations of Martí-Vidal et al. (2011) at $t = 14$ days and our observations at $t = 179$ days the observed proper motion corresponds to a velocity of $9600 \pm 10500 \text{ km s}^{-1}$, not significantly different from zero. We note that large proper motions of the center of the emission region are not expected: the best-determined case is SN 1993J, where a peculiar motion of only $320 \pm 160 \text{ km s}^{-1}$ was observed (Bietenholz et al. 2001).

As mentioned, Chevalier & Soderberg (2010) have suggested that type IIb supernovae are divided into two

categories according to whether the progenitor was extended or compact. Since SN 2011dh had a compact progenitor (Soderberg et al. 2011; Krauss et al. 2012), it would belong to the latter category. According to Chevalier & Soderberg (2010) this category is characterized by a high expansion velocity as well as by variations in the light curve, and presumably also the deceleration, due to episodic mass-loss from the progenitor. SN 2011dh’s relatively high expansion velocity has already been noted, and is confirmed by our VLBI observations. It will, however, be important to continue observations of SN 2011dh’s radio SED as well as VLBI imaging for as long as possible to determine whether the remainder of the predictions are borne out, and to increase our sample of supernovae with observationally determined expansion curves as well as radio and X-ray light curves, since supernovae as nearby and as radio-bright as SN 2011dh are rare events.

Research at York University was partly supported by NSERC. A. B. was supported by a Marie Curie Outgoing International Fellowship (FP7) of the European Union (project number 275596). L.C. is a Jansky Fellow at the NRAO. We thank NRAO for scheduling these target-of-opportunity observations. Our results are partly based on observations with the 100-m telescope of the MPIfR (Max-Planck-Institut für Radioastronomie) at Effelsberg. We made use of the Swinburne University of Technology software correlator, developed as part of the Australian Major National Research Facilities Programme and operated under license. In addition, we also

made use of NASA's Astrophysics Data System Bibliographic Services.

REFERENCES

- Arcavi, I. et al. 2011, *ApJ*, 742, L18, 1106.3551
- Bartel, N., & Bietenholz, M. F. 2008, *ApJ*, 682, 1065, arXiv:0806.3482
- Bartel, N. et al. 2002, *ApJ*, 581, 404
- Bartel, N., Bietenholz, M. F., Rupen, M. P., & Dwarkadas, V. V. 2007, *ApJ*, 668, 924, arXiv:0707.0881
- Berger, E., Kulkarni, S. R., & Chevalier, R. A. 2002, *ApJ*, 577, L5, arXiv:astro-ph/0206183
- Bietenholz, M. 2008, in *The role of VLBI in the Golden Age for Radio Astronomy*. Online at <http://pos.sissa.it/cgi-bin/reader/conf.cgi?confid=72>, p.64, 0802.4219
- Bietenholz, M. F., Bartel, N., & Rupen, M. P. 2001, *ApJ*, 557, 770, arXiv:astro-ph/0104156
- . 2003, *ApJ*, 597, 374, arXiv:astro-ph/0307382
- Bietenholz, M. F. et al. 2011a, ArXiv e-prints, 1103.1783
- Bietenholz, M. F., Brunthaler, A., Bartel, N., Chomiuk, L., Rupen, M. P., Soderberg, A., & Zauderer, B. 2011b, *The Astronomer's Telegram*, 3641, 1, 1006.2111
- Bietenholz, M. F. et al. 2010, *ApJ*, 725, 4
- Brunthaler, A. et al. 2010, *A&A*, 516, A27, 1003.4665
- Brunthaler, A., Reid, M. J., & Falcke, H. 2005, in *Astronomical Society of the Pacific Conference Series*, Vol. 340, *Future Directions in High Resolution Astronomy*, ed. J. Romney & M. Reid, 455, arXiv:astro-ph/0309575
- Chevalier, R. A. 1982, *ApJ*, 258, 790
- . 1998, *ApJ*, 499, 810
- Chevalier, R. A., & Fransson, C. 2006, *ApJ*, 651, 381, arXiv:astro-ph/0607196
- Chevalier, R. A., & Soderberg, A. M. 2010, *ApJ*, 711, L40, 0911.3408
- Deller, A. T. et al. 2011, *PASP*, 123, 275, 1101.0885
- Feldmeier, J. J., Ciardullo, R., & Jacoby, G. H. 1997, *ApJ*, 479, 231, arXiv:astro-ph/9611041
- Fey, A. L., Gordon, D., & Jacobs, C. S., eds. 2009, *IERS Technical Note*, Vol. 35, *The Second Realization of the International Celestial Reference Frame by Very Long Baseline Interferometry* (Frankfurt: Verlag des Bundesamts für Kartographie und Geodäsie), 1
- Griga, T. et al. 2011, *Central Bureau Electronic Telegrams*, 2736, 1
- Horesh, A. et al. 2011a, *The Astronomer's Telegram*, 3411, 1
- Horesh, A., Zauderer, A., & Carpenter, J. 2011b, *The Astronomer's Telegram*, 3405, 1
- Kettenis, M., van Langevelde, H. J., Reynolds, C., & Cotton, B. 2006, in *Astronomical Society of the Pacific Conference Series*, Vol. 351, *Astronomical Data Analysis Software and Systems XV*, ed. C. Gabriel, C. Arviset, D. Ponz, & S. Enrique, 497
- Krauss, M. I. et al. 2012, ArXiv e-prints, 1201.0770
- Law, N. M. et al. 2009, *PASP*, 121, 1395, 0906.5350
- Maddox, L. A., Cowan, J. J., Kilgard, R. E., Schinnerer, E., & Stockdale, C. J. 2007, *AJ*, 133, 2559, arXiv:astro-ph/0702310
- Marion, G. H. et al. 2011, *The Astronomer's Telegram*, 3435, 1
- Martí-Vidal, I., Ros, E., Pérez-Torres, M. A., Guirado, J. C., Jiménez-Monferrer, S., & Marcaide, J. M. 2010, *A&A*, 515, A53, 1003.2368
- Martí-Vidal, I. et al. 2011, *A&A*, 535, L10, 1110.5311
- Maund, J. R. et al. 2011, *ApJ*, 739, L37, 1106.2565
- Pérez-Torres, M. A. et al. 2005, *MNRAS*, 360, 1055, arXiv:astro-ph/0504647
- Perley, R. A., Chandler, C. J., Butler, B. J., & Wrobel, J. M. 2011, *ApJ*, 739, L1, 1106.0532
- Reid, M. J., & Brunthaler, A. 2004, *ApJ*, 616, 872, arXiv:astro-ph/0408107
- Roming, P. W. A. et al. 2009, *ApJ*, 704, L118, 0909.0967
- Ryder, S. D., Sadler, E. M., Subrahmanyan, R., Weiler, K. W., Panagia, N., & Stockdale, C. 2004, *MNRAS*, 349, 1093, arXiv:astro-ph/0401135
- Silverman, J. M., Filippenko, A. V., & Cenko, S. B. 2011, *The Astronomer's Telegram*, 3398, 1
- Soderberg, A. M., Chevalier, R. A., Kulkarni, S. R., & Frail, D. A. 2006, *ApJ*, 651, 1005, arXiv:astro-ph/0512413
- Soderberg, A. M. et al. 2011, ArXiv e-prints, 1107.1876
- Van Dyk, S. D. et al. 2011, *ApJ*, 741, L28, 1106.2897
- Vinkó, J. et al. 2012, *A&A*, 540, A93, 1111.0596